Chiroptical properties of glucose-substituted poly(*p*-phenylene-ethynylene)s in solution and aggregate state

Gennaro Pescitelli, Omar Hassan Omar, Alessandra Operamolla, Gianluca M. Farinola, Lorenzo Di Bari

Supporting Information

Contents

Experimental Section

General procedures

^{1}H-NMR spectra were recorded in $CDCl_3$ at 500 MHz, using the residual proton peaks of $CDCl_3$ at 7.26 ppm as reference. Polymer **AP** and oligomer **HO** average molecular weights were determined by gel-permeation chromatography at 25 °C, with THF as solvent and a 5 μ Mixed-D 300 mm x 7.5 mm column, using polystyrene standards for calibration. UV-vis absorption and circular dichroism (CD) spectra of polymers **AP** and **HO** were recorded using solutions of concentrations around 0.1 mM and 0.5-1 cm quartz cells. Thin films were obtained by slow evaporation of concentrated chloroform solutions in a chloroform-saturated atmosphere.

Alternate copolymer (AP)

^{1}H NMR (500 MHz, $CDCl_3$): δ 0.80÷0.90 (m, 6H), 1.20÷1.60 (m, 24H), 1.80÷2.20 (m, 24H), 3.80÷4.40 (m, 8H), 5.00÷5.50 (m, 8H), 7.13 (bs, 2H), 7.20 (bs, 2H) ppm. Spectrum shown in Figure S7.

Homo-oligomer (HO)

^{1}H NMR (500 MHz, $CDCl_3$): δ 1.90÷2.30 (bs, 24H), 4.15÷4.75 (m, 4H), 5.05÷5.70 (m, 8H), 7.30÷7.50 (m, 4H) ppm. Spectrum shown in Figure S8.

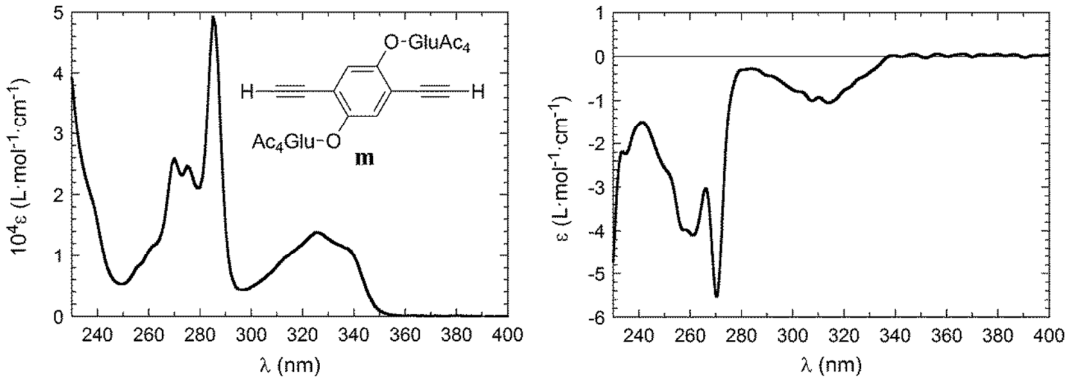

Figure S1. UV (left) and CD (right) spectra for the compound **m** shown in the inset (0.58 mM in chloroform).

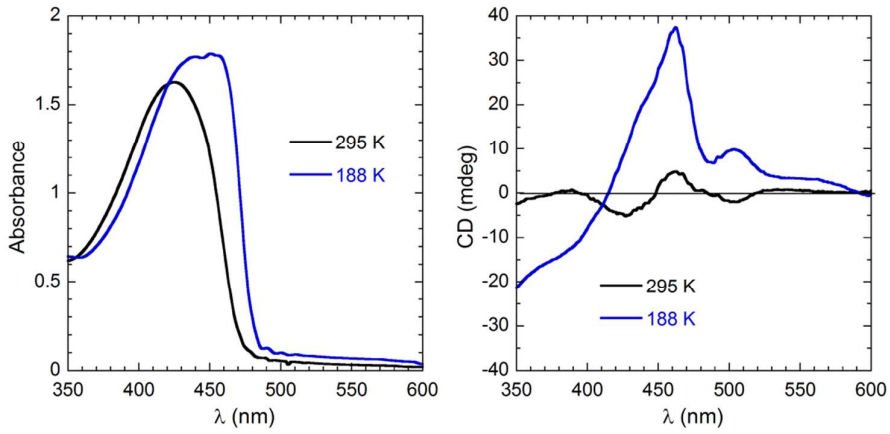

Figure S2. Variable-temperature UV (left) and CD (right) spectra of alternate copolymer **AP** (0.7 mg/mL in dichloromethane). The solvent baseline was recorded at 295 K.

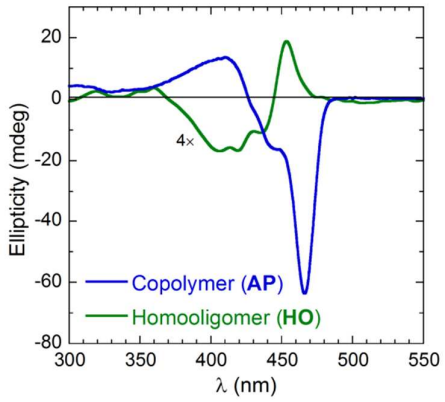

Figure S3. CD spectra of alternate copolymer **AP** and homooligomer **HO** measured on thin films obtained by slow solvent evaporation from concentrated solutions in chloroform.

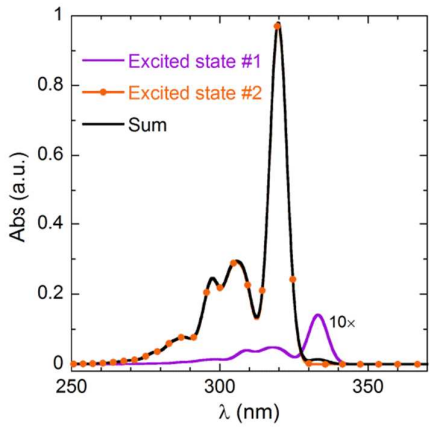

Figure S4. Calculated vibrationally-resolved UV spectrum with TDDFT method (CAM-B3LYP/TZVP) for 1,4-bis(phenylethynyl)benzene dimer (face-to-face arrangement at 6 Å, twist angle τ=-15°). A Gaussian bandshape with 650 cm^{-1} half-height width has been applied. The black spectrum is a sum of the two colored ones.

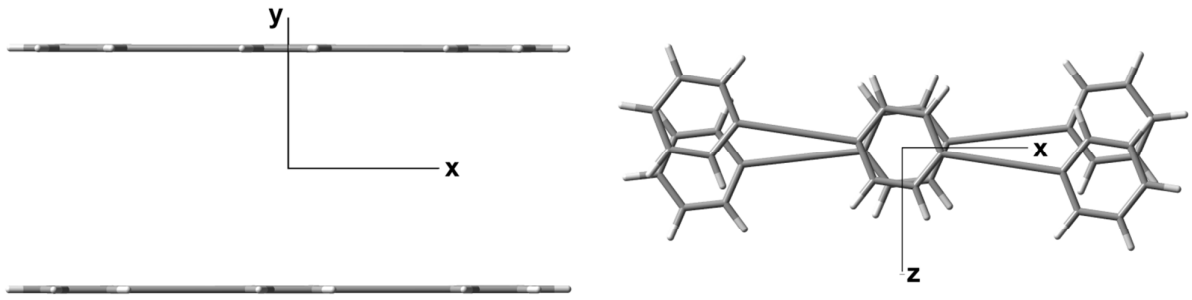

Figure S5. CAM-B3LYP optimized geometry for D_2-symmetric 1,4-bis(phenylethynyl)benzene dimer (face-to-face distance 6 Å, twist angle $\tau = -15°$), seen from two viewpoints.

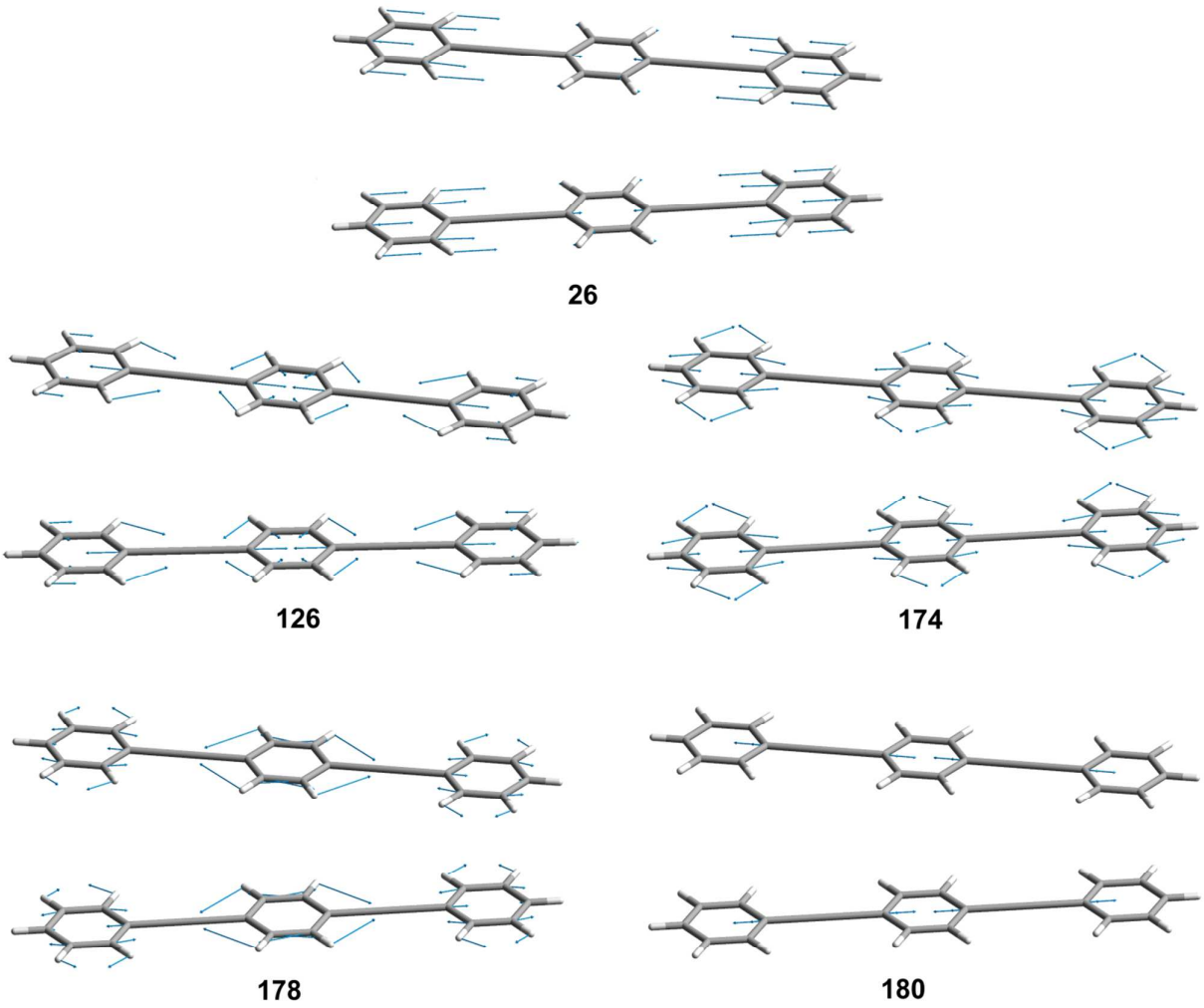

Figure S6. Displacements vectors for selected normal modes computed for the 1,4-bis(phenylethynyl) benzene dimer, geometry shown in Figure S5, with CAM-B3LYP/TZVP.

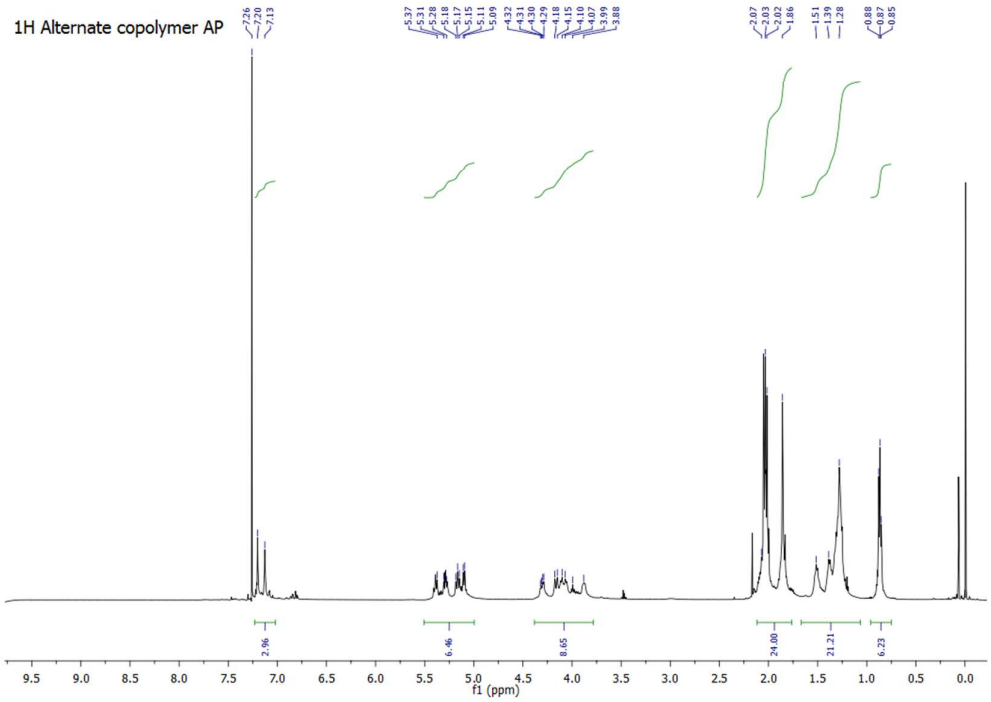

Figure S7. ^{1}H NMR spectrum (500 MHz) of alternate copolymer **AP** in $CDCl_3$.

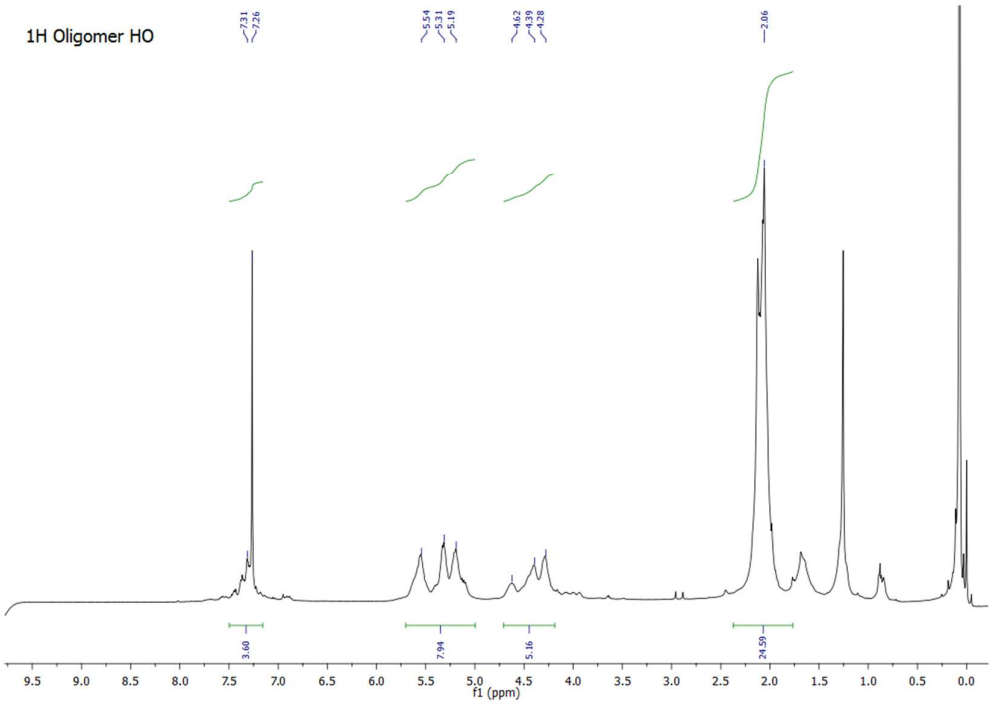

Figure S8. ^{1}H NMR spectrum (500 MHz) of homooligomer **HO** in $CDCl_3$.

Transition	Symmetry	Energy [eV]	Wavelength [nm]	Oscillator strength (*f*)	Polarization (see Figure S5)
#1	B1	3.896	318.2	0.060	z
#2	B3	3.988	310.9	3.572	x

Table S1. Computed parameters for the first two vertical excitations of the 1,4-bis(phenylethynyl)benzene dimer, geometry shown in Figure S5, with CAM-B3LYP/TZVP.

Transition (normal mode)	Energy [eV]	Vibration frequency [cm^{-1}]	Intensity [a.u.]
Excited state #1			
0-0	3.716	-	–0.56
0-1 (26)	3.738	171	–0.18
0-1 (126)	3.861	1171	–0.11
0-1 (174)	3.924	1677	–0.09
0-1 (176)	3.926	1690	–0.04
0-1 (180)	4.009	2363	–0.12
Excited state #2			
0-0	3.873	-	0.67
0-1 (26)	3.894	171	0.18
0-1 (126)	4.018	1171	0.12
0-1 (174)	4.081	1677	0.09
0-1 (176)	4.083	1690	0.04
0-1 (180)	4.166	2363	0.13

Table S2. Computed vibronic transitions for the first two excitations of the 1,4-bis(phenylethynyl) benzene dimer, geometry shown in Figure S5, with CAM-B3LYP/TZVP and FCClasses. Only the transitions with absolute intensity > 0.04 are shown. The normal mode displacement vectors for the first excitation are shown in Figure S6; the vectors for the second excitation are consistent.

Computational Procedures

All calculations were run with Gaussian'09, [1] using default grids and convergence criteria, using the long range corrected hybrid functional CAM-B3LYP[2] and the triple-ζ split-valence basis set with polarization functions TZVP.[3]

The dimer of 1,4-bis(phenylethynyl)benzene (**BPEB**) was built starting from a single D_{2h}-symmetric **BPEB** molecule which was optimized with CAM-B3LYP/TZVP. Two optimized molecules of **BPEB** were then arranged two molecules in a face-to-face arrangement at a distance of 6 Å and a twist angle $\tau = -15°$, as shown in Figure S5, and re-optimized. At this distance and with default convergence criteria, the dimer geometry optimization converged after a single cycle without distorting each **BPEB** from planarity or altering the intermolecular distance; the dimer had D_2 geometry. This geometry was then employed in the following set of calculations, all run with CAM-B3LYP/TZVP. The excited states were computed with TDDFT, including first 6 states and then 2 states, and checking for their consistency; the data for the calculated vertical excitations are summarized in Table S1. Normal modes and vibrational frequencies for the ground state were evaluated with frequency calculations, computing the second derivatives of the energy analytically. The energy gradient of the excited states at the ground state geometry was evaluated by forces calculations.

Vibrationally-resolved UV-vis absorption and CD spectra were calculated according to the linear coupling model (also known as vertical gradient, VG) and the Franck-Condon approximation,[4] using the program **FC***Classes* developed by Fabrizio Santoro.[5-7] The program evaluates the most relevant vibronic component for each electronic transition by partitioning vibronic transitions in "classes", depending on the number of simultaneously excited modes (see http://village.pi.iccom.cnr.it/it/Software). Vibrationally-resolved spectra were calculated for the first two excitations of the **BPEB** dimer, which corresponded to the two in-phase and out-of-phase exciton-coupled components of the HOMO-LUMO π-π* transitions relative to each **BPEB** molecule. Spectra were generated as sums of Gaussians (with 650 cm^{-1} half-height width) applied to individual vibronic components. The analysis of the vibrations most contributing to the resultant spectra is shown in Table S2 and Figure S5.

References

(1) Frisch, M. J.; Trucks, G. W.; Schlegel, H. B.; Scuseria, G. E.; Robb, M. A.; Cheeseman, J. R.; Scalmani, G.; Barone, V.; Mennucci, B.; Petersson, G. A.; Nakatsuji, H.; Caricato, M.; Li, X.; Hratchian, H. P.; Izmaylov, A. F.; Bloino, J.; Zheng, G.; Sonnenberg, J. L.; Hada, M.; Ehara, M.; Toyota, K.; Fukuda, R.; Hasegawa, J.; Ishida, M.; Nakajima, T.; Honda, Y.; Kitao, O.; Nakai, H.; Vreven, T.; Montgomery, J. A.; Peralta, J. E.; Ogliaro, F.; Bearpark, M.; Heyd, J. J.; Brothers, E.; Kudin, K. N.; Staroverov, V. N.; Kobayashi, R.; Normand, J.; Raghavachari, K.; Rendell, A.; Burant, J. C.; Iyengar, S. S.; Tomasi, J.; Cossi, M.; Rega, N.; Millam, J. M.; Klene, M.; Knox, J. E.; Cross, J. B.; Bakken, V.; Adamo, C.; Jaramillo, J.; Gomperts, R.; Stratmann, R. E.; Yazyev, O.; Austin, A. J.; Cammi, R.; Pomelli, C.; Ochterski, J. W.; Martin, R. L.; Morokuma, K.; Zakrzewski, V. G.; Voth, G. A.; Salvador, P.; Dannenberg, J. J.; Dapprich, S.; Daniels, A. D.; Farkas; Foresman, J. B.; Ortiz, J. V.; Cioslowski, J.; Fox, D. J. *Gaussian 09, Revision A.02*, Wallingford CT, 2009.

(2) Yanai, T.; Tew, D. P.; Handy, N. C. *Chem. Phys. Lett.* **2004,** *393*, 51-57.

(3) Schäfer, A.; Huber, C.; Ahlrichs, R. *J. Chem. Phys.* **1994,** *100*, 5829-5835.

(4) Bloino, J.; Biczysko, M.; Santoro, F.; Barone, V. *J. Chem. Theory Comput.* **2010,** *6*, 1256-1274.

(5) Santoro, F.; Barone, V. *Int. J. Quantum Chem.* **2010,** *110*, 476-486.

(6) Santoro, F.; Improta, R.; Lami, A.; Bloino, J.; Barone, V. *J. Chem. Phys.* **2007,** *126*, 084509.

(7) Santoro, F.; Improta, R.; Lami, A.; Bloino, J.; Barone, V. *J. Chem. Phys.* **2007,** *126*, 169903.